

RESEARCH

Open Access



Diagnostic utility of three Tesla diffusion tensor imaging in prostate cancer: correlation with Gleason score values

Rasha Taha Abouelkheir^{1*} , Yasmin Ibrahim Aboshamia¹ and Saher Ebrahim Taman²

Abstract

Background: Preoperative assessment of prostate cancer (PCa) aggressiveness is a prerequisite to provide specific management options. The Gleason score (GS) obtained from prostatic biopsy or surgery is crucial for the evaluation of PCa aggressiveness and personalized treatment planning. Diffusion tensor imaging (DTI) provides valuable information about microstructural properties of prostatic tissue. The most common prostate DTI measures are the fractional anisotropy (FA) and median diffusivity (MD) can give more information regarding the biophysical characteristics of prostate tissue. We aimed to explore the correlation of these DTI parameters with GS levels in PCa patients that can affect the management protocol of PCa.

Results: The computed area under curve (AUC) of the FA values used to differentiate cancer patients from control group was (0.90) with cutoff point to differentiate both groups were ≥ 0.245 . The computed sensitivity, specificity, positive and negative predictive values were (84%, 80%, 95.5%, and 50%), respectively, with accuracy 83.3%. FA showed high positive correlation with Gleason score (p value < 0.001). Median diffusivity (MD) showed negative correlation with GS with statistically significant results (p value $= 0.013$). PCa fiber bundles were dense, orderly arranged, without interruption in the low grade, and slightly disorganized in the intermediate group. However, in the high-grade group, the fiber bundles were interrupted, irregularly arranged, and absent at the site of cancerous foci.

Conclusions: Combined quantitative parameter values (FA and MD values) and parametric diagrams (FA and DTI maps) can be utilized to evaluate prostate cancer aggressiveness and prognosis, helping in the improvement of the management protocol of PCa patients.

Keywords: Fractional anisotropy, Mean diffusivity, Prostate cancer, Diffusion tensor imaging, Gleason score

Background

According to the Global Cancer Statistics 2020, prostate cancer (PCa) is the 2nd non-cutaneous leading cause of cancer death in men, and the 4th most commonly diagnosed cancer [1].

Although different diagnostic tools are prevalent for diagnosis of males suspected to have prostatic cancer, as

serum prostate-specific antigen (PSA) levels, transrectal ultrasound (TRUS), and digital rectal examination, the sensitivity and specificity of all these modalities in the early diagnosis of PCa are limited [2].

Generally, the perfect imaging tool in the prostate cancer diagnosis is MRI, because of its great spatial resolution and the outstanding contrast of soft tissue. On the other hand, its routine sequences show moderate specificity and sensitivity for the prostate cancer diagnosis [3, 4].

Diffusion tensor imaging (DTI) is a diffusion weighted image (DWI) extension where the diffusion of water directional dependence can be examined in at least 6

*Correspondence: rashataha2020@gmail.com; Dr_rasha_taha@mans.edu.eg

¹ Radiology Department, Urology and Nephrology Center, Mansoura University, Mansoura, Egypt
Full list of author information is available at the end of the article

directions [5]. This technique is a tensor and gives extra-structural data about the anisotropy and magnitude of diffusion of water in tissues [6, 7].

The prostate contains histologically dissimilar structures. This leads to diffusion anisotropy, because the restriction of diffusion is dissimilar in different directions [8]. DTI can be helpful in providing more information concerning the prostate biophysical characteristics [6]. It can give both values of fractional anisotropy (FA) and mean diffusivity (MD) that may reveal the physiologic and pathologic alterations [9, 10].

Prostate cancer diagnosis is supposed if the levels of PSA are increased more than 4 ng/mL [11]. The diagnostic work-up of patients with an elevated PSA level and an increased risk of PCa is continuously changing. Histopathologic verification via a systematic TRUS-guided biopsy is the standard clinical procedure to confirm the diagnosis of PCa [12].

Gleason score (GS) analysis was utilized to assess the grade of tumor and the patient's prognosis who suffer from prostate cancer utilizing samples from a biopsy from the prostate [13]. The total score was established on the microscopic picture of cells. Half of the score is established on the commonest cell morphology appearance (scored 1–5) and the other half is established on the 2nd commonest cell morphology appearance (scored 1–5) [14].

Clinically significant PCa is defined on pathology/histology as Gleason ≥ 7 (including 3+4 with prominent but not predominant Gleason 4 component), and/or volume ≥ 0.5 cc and/or have extra prostatic extension [15, 16].

The correlation between functional parameters as assessed by DTI and the aggressiveness of prostate cancer determined by Gleason score (GS) may add a value in the prediction of prostate cancer pathological grading and distinguish clinically significant prostate cancer from indolent prostate cancer noninvasively to enhance the choice of a proper management and evaluation of the prognosis of the patient [3, 6].

The objective of this prospective study was to investigate the correlation between diffusion tensor imaging parameters with Gleason score values in PCa patients that can affect the management protocol of PCa.

Methods

Institutional review board was obtained for this prospective study done from July 2020 to March 2022. Informed consents were obtained from all patients and controls before MRI examination was done. The study was conducted on 83 consecutive male cases. Their ages ranged

from (35–86 years) and their mean age was about (67 ± 7) years old.

Inclusion criteria

The study included patients who were clinically suspected to have prostate cancer by digital rectal examination or by high serum PSA level (>4 ng/ML). Patients did not undergo previous hormonal, radio-therapeutic management, or chemotherapy prior to the MRI studies. No biopsies were taken in all patients prior to the MRI examinations.

Exclusion criteria

Patients with general contraindications to do MRI as patients with cardiac pacemaker, cochlear implant, patients with motion artifact that leads to poor MR images quality, patients with prior hormonal, surgical, or irradiation therapies for prostate cancer. Pathologically proven lesions other than prostatic adenocarcinoma like prostatitis or BPH are excluded.

Thirteen patients were excluded from the study. One patient was claustrophobic and did not complete the study. Two patients showed images with motion artifacts, eight patients with multiple benign prostatic hyperplasia (BPH) nodules at the transitional zone and two patients with prostatitis.

Patient group ($N=50$) with clinically suspected prostatic lesions their mean age (67 ± 7) years old and 20 healthy volunteers their mean age (66 ± 8) years old which were defined as control group, they were coming for MRI examinations due to other causes rather than prostatic disease. Patients were referred from the outpatient clinic of Urology and Nephrology Center, Mansoura University. Only patients with final histopathological diagnosis after biopsy were included. Ethics Committee of the faculty of medicine, University of Mansoura approved the study protocol.

Image acquisition

Routine MRI together with DTI was carried out for patients and control groups using a 3-T MRI scanner (Ingenia, Philips medical systems, Veenpluis, Netherlands), imaging in the supine position using phased-array body coil. The field of view (FOV) was taken from the iliac crest to the end of symphysis pubis. The bladder, prostate, and the surrounding structures were included and well delineated. The following sequences were done, Axial T1WI: to exclude presence of any hemorrhagic foci. FOV=200 mm. TR (repetition time)=400 ms. TE (echo time)=9 ms. Slice thickness=3 mm. Slice interval=0.3 mm. T2WI, in axial, coronal, and sagittal planes: the gold standard sequence to demonstrate

prostatic anatomy FOV=200 mm. TR=5000 ms. TE=110 ms. Slice thickness=3 mm. No interslice gap, and matrix: 288×192 . DWI: to evaluate any abnormally restricted diffusion seen within the prostate: TE=85 ms. TR=7255 ms. FOV=200 mm. Slice thickness 3 mm. Two b values were used (zero and 1400 s/mm^2). DTI: using single-shot echo planner-imaging sequences. Matrix: 152×152 . TR=10,000 ms. TE=100 ms. Number of averages: 1. Slice thickness=4 mm. No gap. FOV=260 X 260 mm^2 . Two b values were used: (0 and 1400 s/mm^2). Acquisition time=6 min. NSA=three. Flip angle=90°. Number of directions=32.

Image interpretation

MR images were analyzed by 2 radiologists (YA and RA) with 5- and 15-year experience in uro-radiology and agreed by consensus. They were blinded to the histopathological results. Qualitative analysis was done to the prostate gland to detect the lesions of abnormal low

signal intensity (SI) on T2 and restricted signals on DWI, also to detect the integrity of the capsule of the prostate and the extension of the tumors to the adjacent structures as well as the periprostatic fat planes.

Post-processing

Following image acquisition, all images were stored in DICOM format, then transferred to a digital workstation (Intellispace portal Workspace 6.0.1 Philips medical systems Netherlands B.V) supplied by the vendor, for processing. Metrics were measured within the detected lesions using region of interest (ROI) method. ROI placement corresponds to the most restricted area in diffusion weighted image, excluding areas of calcification and hemorrhage. (Median ROI area, 0.81 cm^2 , range, 0.4–2 cm^2). Each ROI was scanned three times, and the average value was used as the final FA and MD value. FA and MD values were registered in excel sheet. Parametric diagrams (FA and DTI maps) were obtained.

Table 1 Validity of MD & FA in discriminating patients with prostate cancer from the control group

	AUC (95% CI)	p value	Cut off point	Sensitivity (%)	Specificity (%)	PPV (%)	NPV (%)	Accuracy (%)
MD	0.95 (0.98–1.0)	<0.001*	≤ 1.075	88.0	90.0	97.8	60	88.3
FA	0.90 (0.769–1.0)	<0.001*	≥ 0.245	84.0	80.0	95.5	50.0	83.3

AUC: area under curve. PPV: positive predictive value. NPV: negative predictive value. *Statistically significant

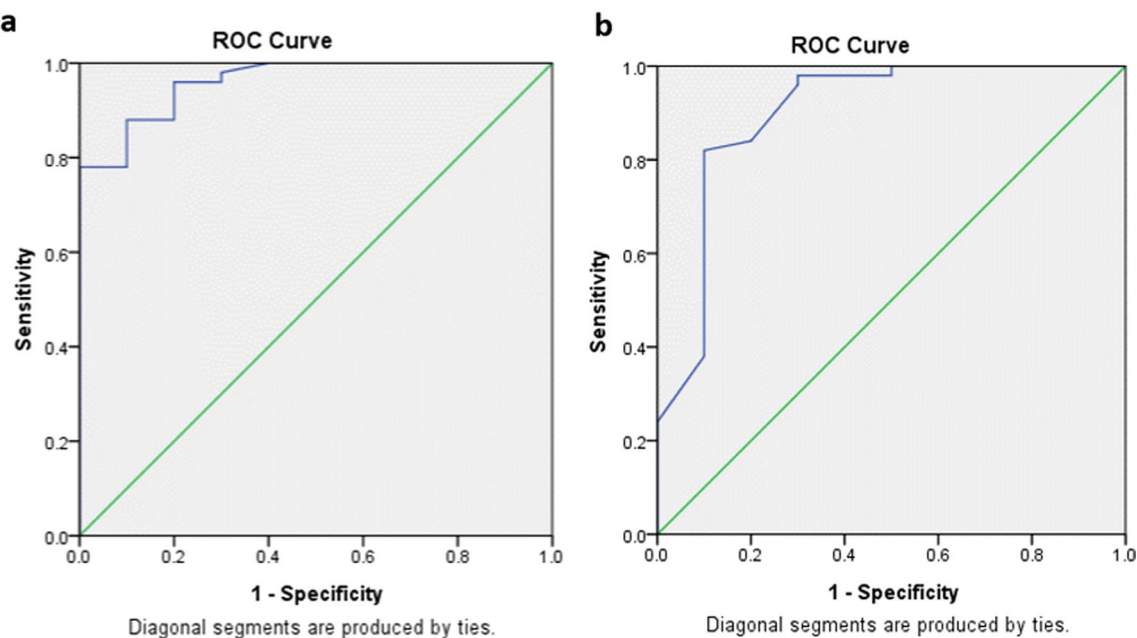


Fig. 1 a ROC curve for MD in discriminating cases from control groups. b ROC curve for FA in discriminating cases from control groups

Table 2 Correlation between Gleason score, PSA level and imaging data FA, MD

		Gleason score	PSA level
FA	R	.744*	.128
	P	< 0.001	.377
MD*10 ⁻³	R	-.347*	-.305*
	P	.013	.031

r: Spearman correlation coefficient *Statistically significant

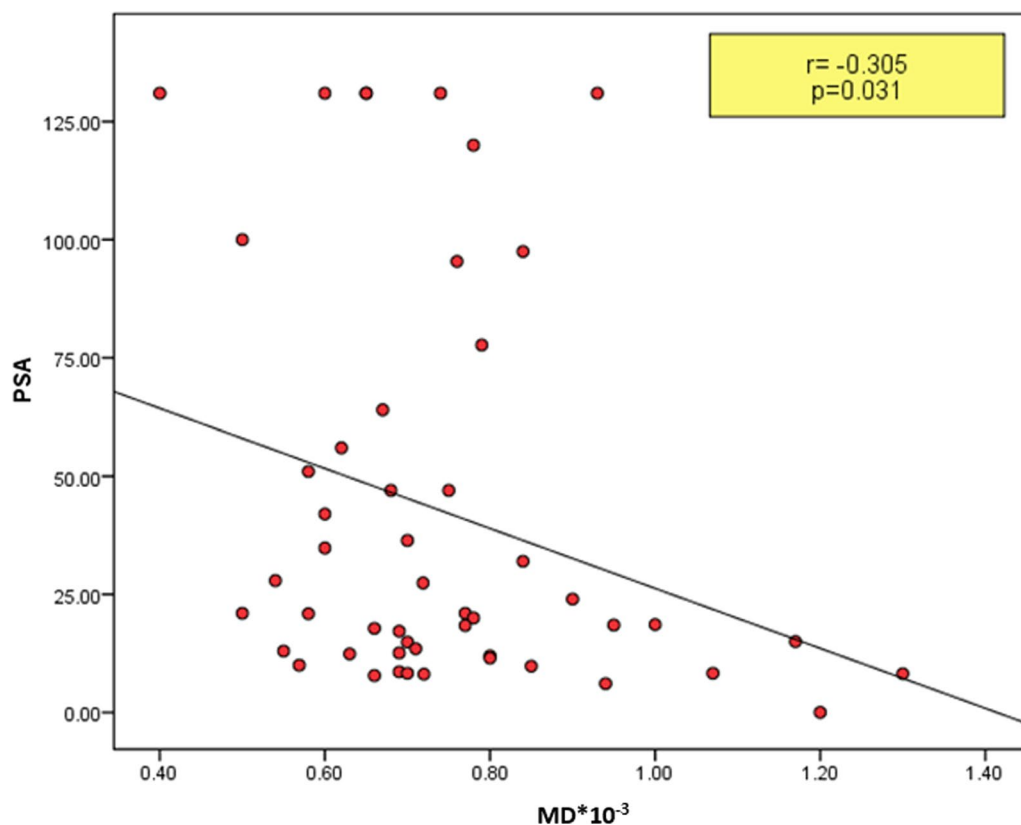
Final diagnosis

After MRI examinations, standard 12-core random systematic TRUS-guided needle biopsy was done for all patient group (50). Histopathological biopsy results were the reference standard. The average estimated duration between the MRI study and the biopsy did not exceed 7 days. TRUS-guided needle biopsy was done, using (Flex focus 500, bk medical, Herlev, Denmark) with high-frequency transrectal transducer (5–9 MHz) and a condom cover. The patient lied in a modified lithotomy position. Anorectal application of a lubricant gel with lidocaine cream was used topically, before insertion of the probe.

Axial scans were used to detect any abnormal lesions at the prostate gland, as well as the seminal vesicles infiltration by the tumors. Then, the twelve cores were taken, and tissue biopsies were sent for histopathologic assessment. When TRUS-guided biopsy was done, and the diagnosis of prostatic carcinoma was confirmed, correlation between the values of DTI parameters (FA and MD), PSA level, pathological results, Gleason score, and final diagnoses of the cases were done.

Statistical analysis and data interpretation

The data were collected, processed, coded, and introduced to the computer to undergo analysis utilizing SPSS program for windows version 22.0. Armonk, NY: IBM Corp. The qualitative results were expressed utilizing percent and number. The DWI map was obtained following scanning. The quantitative results were expressed utilizing median (minimum and maximum) for nonparametric data, and on the other hand, continuous variables were provided as mean \pm SD (standard deviation) for parametric data. Receiver operating characteristic (ROC)

**Fig. 2** Scatter plot diagram shows correlation between PSA level and MD among the studied 50 cases. The PSA level is inversely correlated with MD value. PSA: prostatic specific antigen. MD: median diffusivity

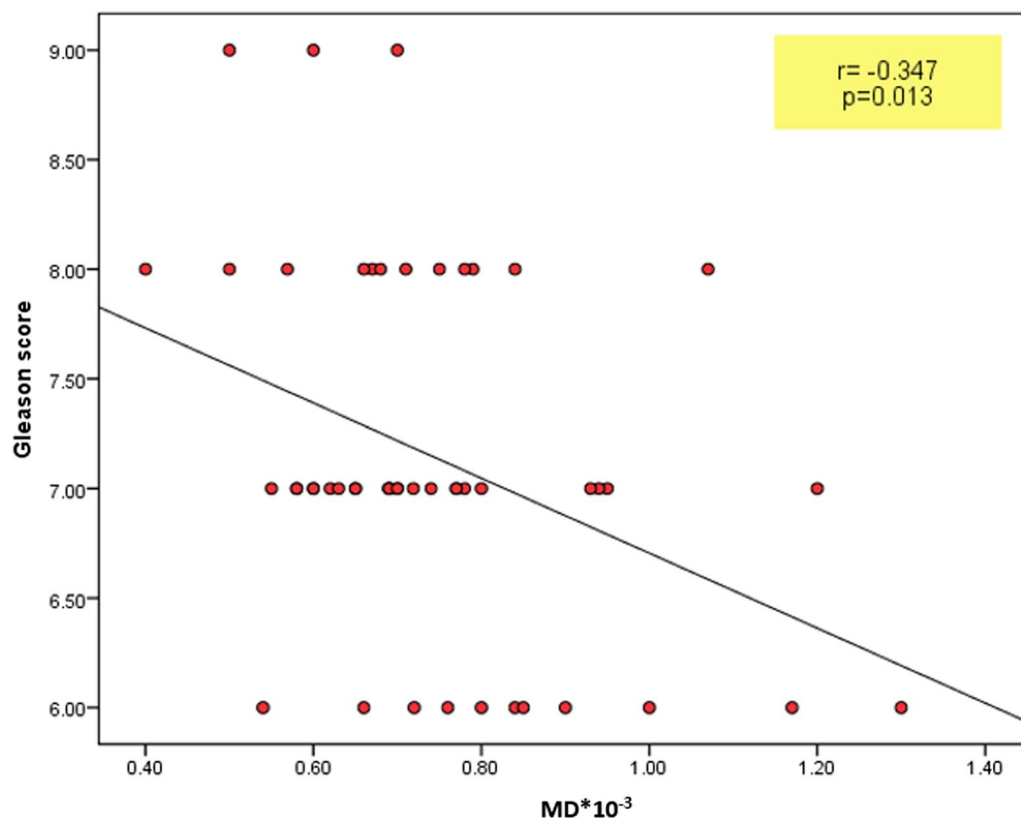


Fig. 3 Scatter plot diagram shows correlation between MD & Gleason score among the 50 studied cases. The Gleason score is inversely correlated with MD value. MD: median diffusivity

curve was used to calculate FA & MD cutoff values with their sensitivity and specificity.

Overall diagnostic accuracy was assessed in terms of the multiclass analysis of the area under the ROC curve (AUC). The level of significance of the collected data was determined as the p value ≤ 0.05 . One-way ANOVA test was utilized to make comparison between Gleason score and DTI metrics (FA, MD). The Spearman's correlation test was used to determine the strength of the relationships between Gleason score, PSA level and imaging data FA, MD.

Results

Patient demographics

This research included 50 male patients; the highest prevalence of prostate cancer among this study population was between 70 and 79 years old. All were clinically suspected of prostate cancer. The PSA level for them ranged from 6 to 131 ng/dl (mean \pm SD = 35 ± 34 ng/dl), with median value about 20.95 ng/ml. The main level at presentation time was less than 30 ng/ml.

Out of the 50 patients subjected to this study, 23 patients (46%) had obstructive irritative lower urinary

tract symptoms, 12 patients (24%) incidentally discovered high PSA, 8 patients (16%) had hematuria, 4 patients (8%) had indwelling of urethral catheter, 2 patients (4%) had bone aches, and 1 patient (2%) had perianal pain.

According to the tumor location, out of the pathologically proven 50 malignant lesions, 12 lesions were located at the right mid prostate, 16 lesions were located at the left mid prostate, 2 lesions were located at the right prostate apex, 6 lesions were located at the left prostate apex, 3 lesions were located at the right prostate base, 6 lesions were located at the left prostate base, and 5 lesions were simultaneously involving the peripheral and central gland regions.

Histopathological grading: Among the 50 cases of PCa, 11 cases presented with Gleason scores of (3+3=6), which is considered as a low-grade tumor, 24 cases presented with a Gleason score of 7; 11 of score (3+4=7) and 13 of (4+3=7), which is considered as an intermediate grade tumor, 12 cases had Gleason scores of (4+4=8); and 3 cases had Gleason score (5+4=9). Both 8 and 9 groups (15 cases) were considered as a high-grade tumor.

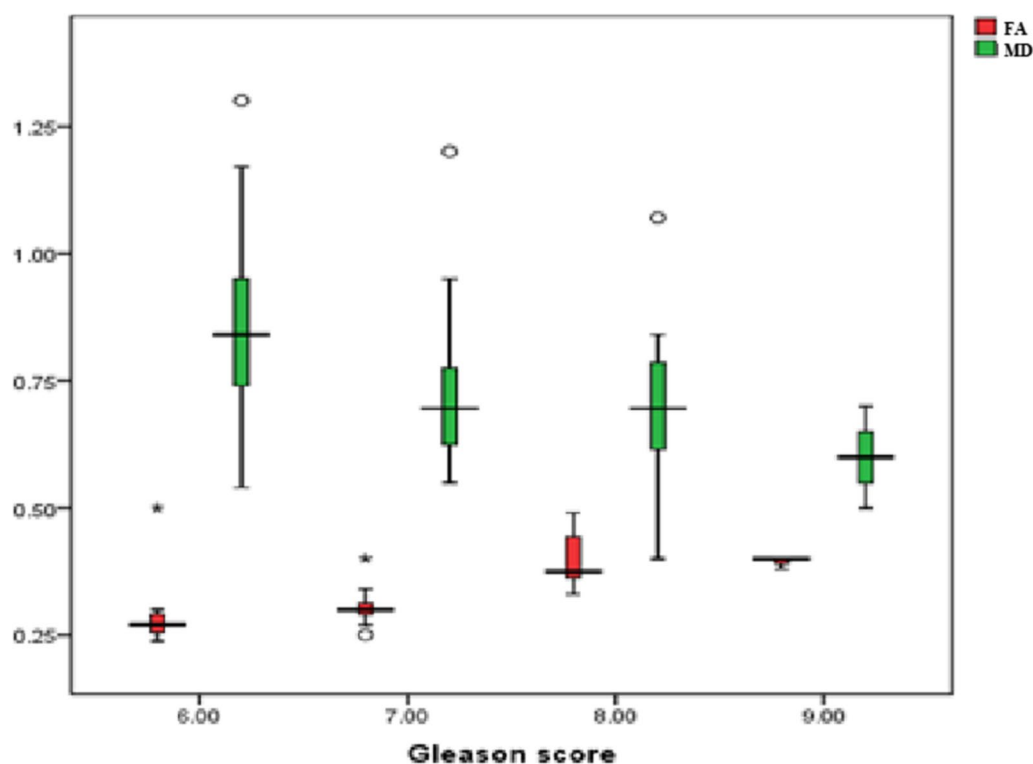


Fig. 4 One-way ANOVA test: FA, MD in correlation with Gleason score among studied patients. FA: fractional anisotropy, MD: median diffusivity

Table 3 Mean DTI metrics values distribution according to Gleason score

	Gleason score	No	Mean	SD	Minimum	Maximum	Test of significance
FA	6	11	.28800	.073185	.238	.500	$F = 15.14$ $p < 0.001^*$
	7	24	.30342	.028255	.250	.400	
	8	12	.39683	.052966	.330	.490	
	9	3	.39333	.011547	.380	.400	
	Total	50	.32784	.064652	.238	.500	
MD	6	11	.8673	.22055	.54	1.30	$F = 2.91$ $p = 0.045^*$
	7	24	.7304	.14992	.55	1.20	
	8	12	.7016	.17153	.40	1.07	
	9	3	.6000	.10000	.50	.70	
	Total	50	.7458	.18083	.40	1.30	

*Statistically significant

(See figure on next page.)

Fig. 5 A 67-year-old male patient, presented with irritative and obstructive lower urinary tract symptoms, his PSA level was 9.8 ng/ml. **a** T2 WI high-resolution pelvic MRI: a well-defined lesion (2 × 1.4 cm) at the right PZ at the level of mid gland with an abnormal hypointense T2WI SI. **b** DWI image showed restricted diffusion. **c** ROI on DTI image: (FA = 0.26), (MD = 0.85 × 10 mm²/sec), **d** DTT map displays dense, orderly arranged fiber bundles without interruption that corresponds with low-grade prostate cancer. **(e)** Transrectal US and biopsy were done: an ill-defined suspicious hypoechogenic focal lesion at the right PZ (red arrow). **f** Histopathological biopsy: prostatic adenocarcinoma, moderately differentiated, combined Gleason score: (3 + 3 = 6). T2WI, T2-weighted imaging; FA, fractional anisotropy; DWI, diffusion-weighted imaging; DTT, diffusion tensor tractography. PZ: peripheral zone

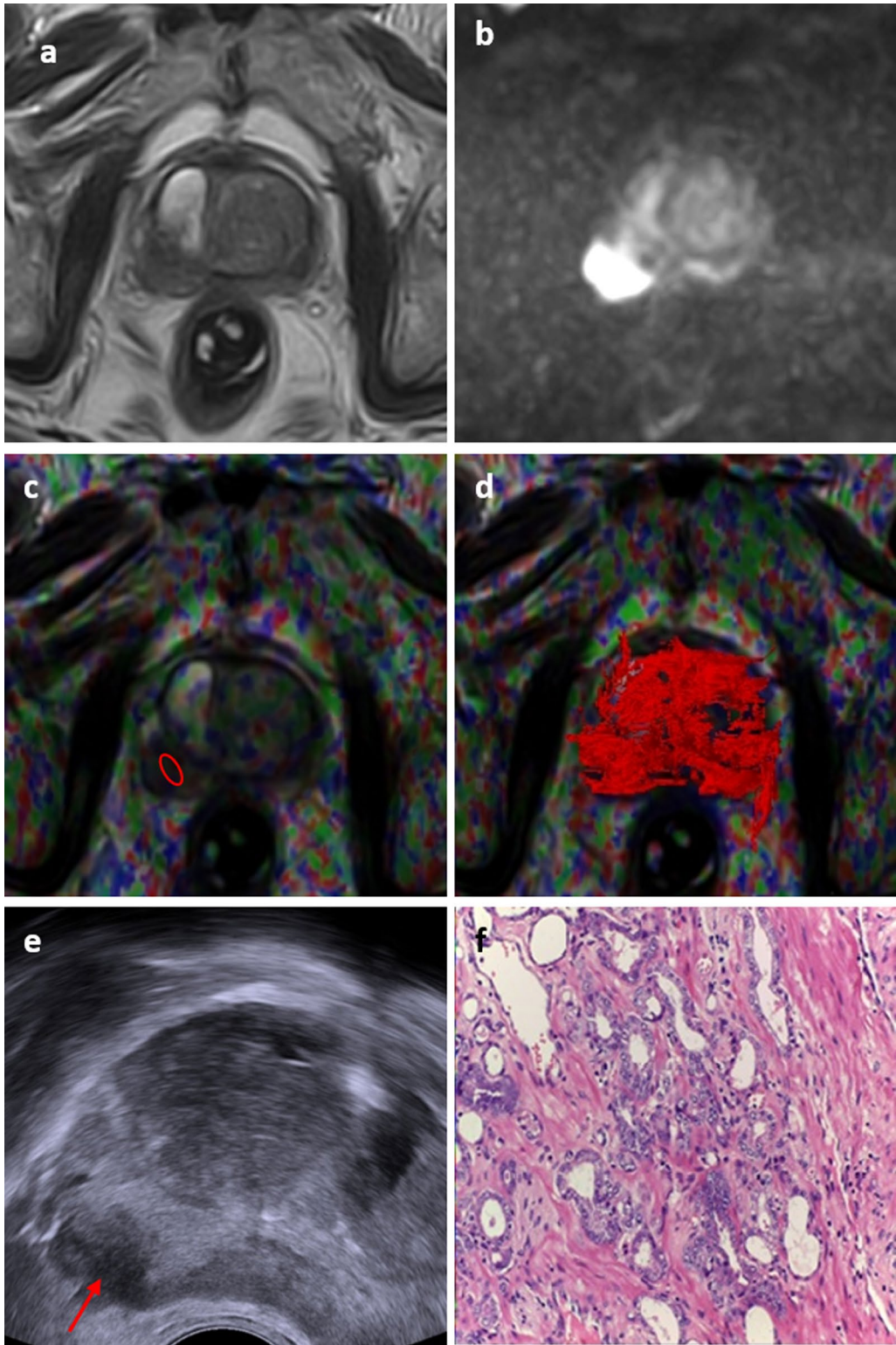


Fig. 5 (See legend on previous page.)

MRI examination

Diffusion tensor imaging metrics

There was a significant decrease in MD values in the cancerous foci in patients versus normal prostatic foci in controls ($p < 0.001$). The measured MD values for the control and patient groups, respectively, were $(1.69 \pm 0.183) \times 10^{-3} \text{ mm}^2/\text{s}$, and $(0.745 \pm 0.180) \times 10^{-3} \text{ mm}^2/\text{s}$, respectively. At ROC curve, the AUC of the MD values used to differentiate, patients from controls were (0.95) with cutoff point to differentiate, both groups were $(\leq 1.075 \times 10^{-3} \text{ mm}^2/\text{s})$. The sensitivity, specificity, positive and negative predictive values were (88%, 90%, 97.8%, and 60% with accuracy 88.3%) (Table 1, Fig. 1a).

There was a significant increase in FA values in the cancerous foci in patients versus normal prostatic foci in controls ($p < 0.001$). The measured mean FA values for the control and patient groups, respectively, were (0.219 ± 0.028) and (0.327 ± 0.06) , respectively. At ROC curve, the AUC of the FA values used to differentiate patients from controls were (0.90) with cutoff point to differentiate both groups were ≥ 0.245 . The computed sensitivity, specificity, positive and negative predictive values were (84%, 80%, 95.5%, and 50%), respectively, with accuracy 83.3% (Table 1, Fig. 1b).

When considering the correlation between Gleason score, PSA and imaging data FA, MD: The FA showed high positive correlation with Gleason score (P value < 0.001) statically significant; however, the FA showed a very low positive correlation with PSA (P value = 0.1): statically insignificant. The MD showed a negative correlation with Gleason score and PSA with statistically significant results (Table 2). Scatter plot diagram is used to mathematically show the relationship between the MD and PSA & Gleason score among the 50 studied cases (Figs. 2, 3).

Considering the mean DTI metrics values distribution (FA, MD) according to Gleason score utilizing one-way ANOVA test (Fig. 4): In the 11 patients of Gleason score (3 + 3 = 6), the mean FA value was (0.28 ± 0.07) and the mean MD value was $(0.86 \pm 0.22 \times 10^{-3} \text{ mm}^2/\text{sec})$. In 24 patients of Gleason score 7, the mean FA value was (0.3 ± 0.02) and the mean MD value was $(0.73 \pm 0.14 \times 10^{-3} \text{ mm}^2/\text{sec})$. In 12 patients of Gleason

score 8, the mean FA value was (0.39 ± 0.05) and mean MD value was $(0.70 \pm 0.17 \times 10^{-3} \text{ mm}^2/\text{sec})$. In 3 patients of Gleason score 9, the mean FA value was (0.39 ± 0.01) and the mean MD value was $(0.6 \pm 0.1 \times 10^{-3} \text{ mm}^2/\text{sec})$ (Table 3).

According to the DTT maps, the PCa fiber bundles were dense, orderly arranged without interruption in the low-grade, slightly disorganized in the intermediate group. However, in the 15 cases of the high-grade group, the fiber bundles were interrupted, irregularly arranged, and absent at the site of cancerous foci.

The characteristic features of the different groups according to the FA, MD, and DTT maps are presented in (Figs. 5, 6, 7).

Discussion

The most significant finding in this study is that the measured DTI anisotropy parameter (FA) and diffusivity parameter (MD) had higher sensitivity and diagnostic accuracy in evaluation of the aggressiveness of prostate cancer in correlation with Gleason score, pathological scoring system, and PSA levels.

This study was carried out on 50 patients. The highest prevalence of prostate cancer among this study population was between (70 and 79 years old); this copes with the recorded age incidence of prostate cancer [8, 17]. Clinically speaking, age is considered a significant non-modifiable risk factor for PCa [18, 19]. Some risk factors of PCa can be affected by aging, such as immunity, cholesterol metabolism, obesity, free testosterone levels, and genetic effects [20].

In prostate cancer, FA and MD vary because of altered diffusivity and disorganization of the fibers. (MD) has been used to describe the strength of diffusion in biological tissues which is valid only for homogeneous fluid with free diffusion, diffusion can be hindered or restricted, and result in decreased MD [21].

Fractional anisotropy defines the degree of anisotropy and reflects the degree of alignment of cellular structures and measures the total magnitude of water directional movement along the fibers [22]. In this study, to be more accurate in determination of the FA and MD, especially in large heterogenous lesions, we used the ROI in the portion of the tumor showing the highest SI

(See figure on next page.)

Fig. 6 A 70-year-old male patient, presented hematuria, his PSA level was 38 ng/ml. **a** T2 WI high-resolution pelvic MRI: a well-defined lesion (2.2 × 1.2 cm) at the right PZ at the level of mid gland with an abnormal hypointense T2WI SI with irregular capsule. **b** DWI image showed restricted diffusion. **c** ROI on DTI image: (FA = 0.31), (MD = $0.55 \times 10 \text{ mm}^2/\text{sec}$). **d** DTT map displays slightly disorganized fiber bundles without interruption that corresponds with intermediate grade prostate cancer. **e** Transrectal US and biopsy were done: an ill-defined suspicious hypoechoic focal lesion at the left PZ (yellow arrow). **f** Histopathological biopsy: prostatic adenocarcinoma, moderately differentiated, combined Gleason score: (3 + 4 = 7). T2WI, T2-weighted imaging; FA, fractional anisotropy; DWI, diffusion-weighted imaging; DTT, diffusion tensor tractography. PZ: peripheral zone

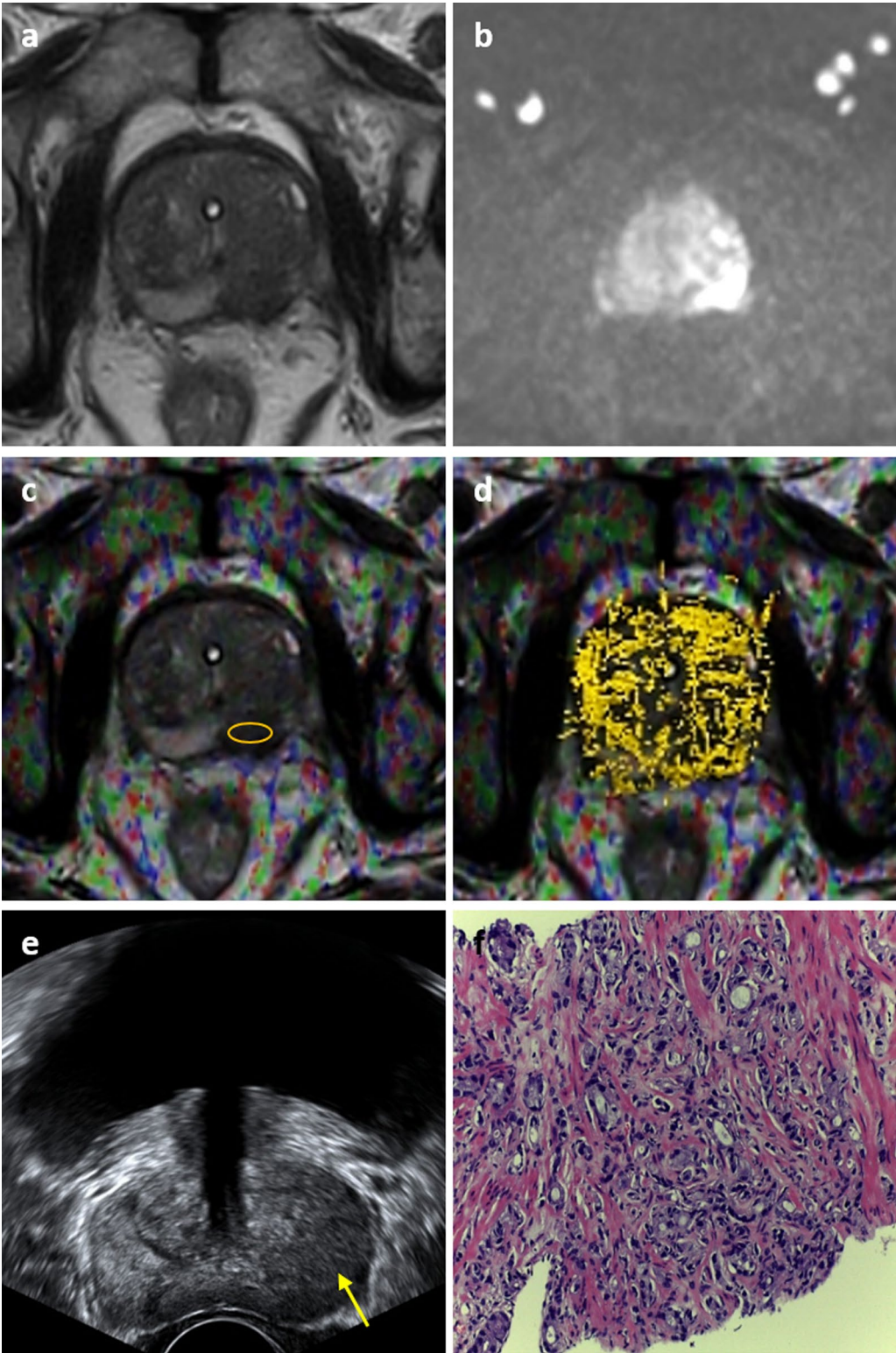


Fig. 6 (See legend on previous page.)

on DWI and the lowest SI on ADC map, compared with the signal from the adjacent tumoral tissue. [23]. We used the ellipse ROI, as it was suggested to be a simpler and appropriate method for MD measurement in PCa [24].

In this study, the mean FA detected among the control group ($N=20$) was (0.219 ± 0.028) ; however, the mean FA among the patient group ($N=50$) was (0.327 ± 0.065) with the cutoff point of FA value among the 70 male included in this study was (≥ 0.245) above which the detected lesion is considered a cancer lesion with 84% sensitivity and 80% specificity.

The mean MD value was detected among control group ($N=20$) $(1.69 \pm 0.183 \times 10^{-3} \text{ mm}^2/\text{sec})$; however, MD value detected among the patient group ($N=50$) was $(0.745 \pm 0.180 \times 10^{-3} \text{ mm}^2/\text{sec})$. The cutoff point of MD value among the 70 males included at this study was (≤ 1.075) below which the detected lesion is considered a cancer.

The greater FA values of cancer lesions than FA values of normal tissues as well as the lesser mean cancerous tissue MD values than the normal values coincide with Onya A., et al. who reported on 2017 that FA of cancerous tissue is higher than of normal tissues [22]. This also agreed with Li L., et al. who concluded on 2015 that elevated FA values and reduced MD values in prostate cancer at 3 T MRI machine [3].

Gholizadeh N., et al. also on 2019 showed reduced diffusivity (MD) and elevated fractional anisotropy (FA) values of cancer foci from several DTI maps suggesting increased cellularity or overcrowded cancerous tissues [6]. This can be explained as the increased intracellular viscosity and the number of cell membranes in cancerous tissues leads to diffusion directionality and restricted diffusion, whereas water diffusion in benign tissue is fairly isotropic with low FA and high MD [25].

This is partially contradicted to the results by Manenti G., et al. on 2007 who detected significant reduction in MD and FA measurements in PZ prostate cancer compared to healthy areas [26]. He related the decreased FA value to the nature of tumorous tissues, which were described as areas of absent or reduced fibers. This can be explained by a shift of the adjacent healthy tissues "fibers." FA values were reduced in the tumor area, contrary to the surrounding healthy tissue, because of

the disorganized structure of the tumor itself (tumoral necrosis or degeneration) [26].

High-grade tumors having high cellularity with packed cells this will have elevated levels of FA; on the other hand, tumors of low grade showing decreased cellularity with cells that are randomly arranged will have decreased FA [3, 7]. Diffusion is more restricted and hindered in the cases of poorly formed/fused/cirribriform glands that significantly reduce MD values in high-grade tumors [27].

PSA level showed decreased specificity in prostate cancer diagnosis, because of its false positive results in benign diseases as prostatitis and BPH; consequently, increased PSA does not essentially demonstrate the presence of PCa [11]. Moreover, its normal level does not rule out the presence of PCa. On the other hand, evaluation of PSA is still utilized because of absence effective biomarkers in detection of PCa [28, 29]. This coincides with our results as PSA showed a statically insignificant very low positive correlation with FA, and a statistically significant negative correlation with MD.

In this study, we found that the FA showed high positive correlation with Gleason score (p value <0.001) which is statically significant. Furthermore, we found that MD showed negative correlation with Glasson score with statistically significant results (p value $=0.013$). These alterations may be because of the progressively dense arrangement of cells in the tumors of high grades; additionally, the extracellular space decreases [17]. This coincides with Tian W, et al. [17] who found nearly the same results.

This is not consistent with Wang S, et al. who reported a negative correlation between the values of FA and Gleason scores, signifying that an elevation in Gleason scores will lead to a slowly decrease in the value of FA [25]. Nezzo M, et al. documented no correlation between the value of FA and Gleason score. This conflict in FA correlation with prostate cancerous tissues may be related to the difference in the parameters of acquisition protocols and/or post-processing techniques [27].

The limitations of this study could be summarized in the small number of patients enrolled in the study, together with absence of follow-up DTI for the patients. No fusion or cognitive biopsy on the suspected lesion was observed. Another limitation of this study was carried

(See figure on next page.)

Fig. 7 A 70-year-old male patient, presented with hematuria, his PSA level was 69 ng/ml. **a** T2 WI high-resolution pelvic MRI: The prostate is seen totally replaced by a soft tissue mass, measuring $(5 \times 3.6 \text{ cm})$ displays an abnormal hypointense T2WI SI with extracapsular extension & infiltration of the left neurovascular bundle as well as the anterior wall of the anal canal. **b** DWI image showed restricted diffusion. **c** ROI on DTI image: (FA = 0.47), (MD = $0.79 \times 10 \text{ mm}^2/\text{sec}$), **d** DTT map displays interrupted, irregularly arranged fiber bundles that corresponds with high-grade prostate cancer. **e** Transrectal US and biopsy were done: an ill-defined heterogeneous soft tissue lesion involving the CZ and PZ with irregular prostatic capsule (green arrow). **f** Histopathological biopsy: prostatic adenocarcinoma, poorly differentiated, combined Gleason score: $(4 + 5 = 9)$. T2WI, T2-weighted imaging; FA, fractional anisotropy; DWI, diffusion-weighted imaging; DTT, diffusion tensor tractography. CZ: central zone, PZ: peripheral zone

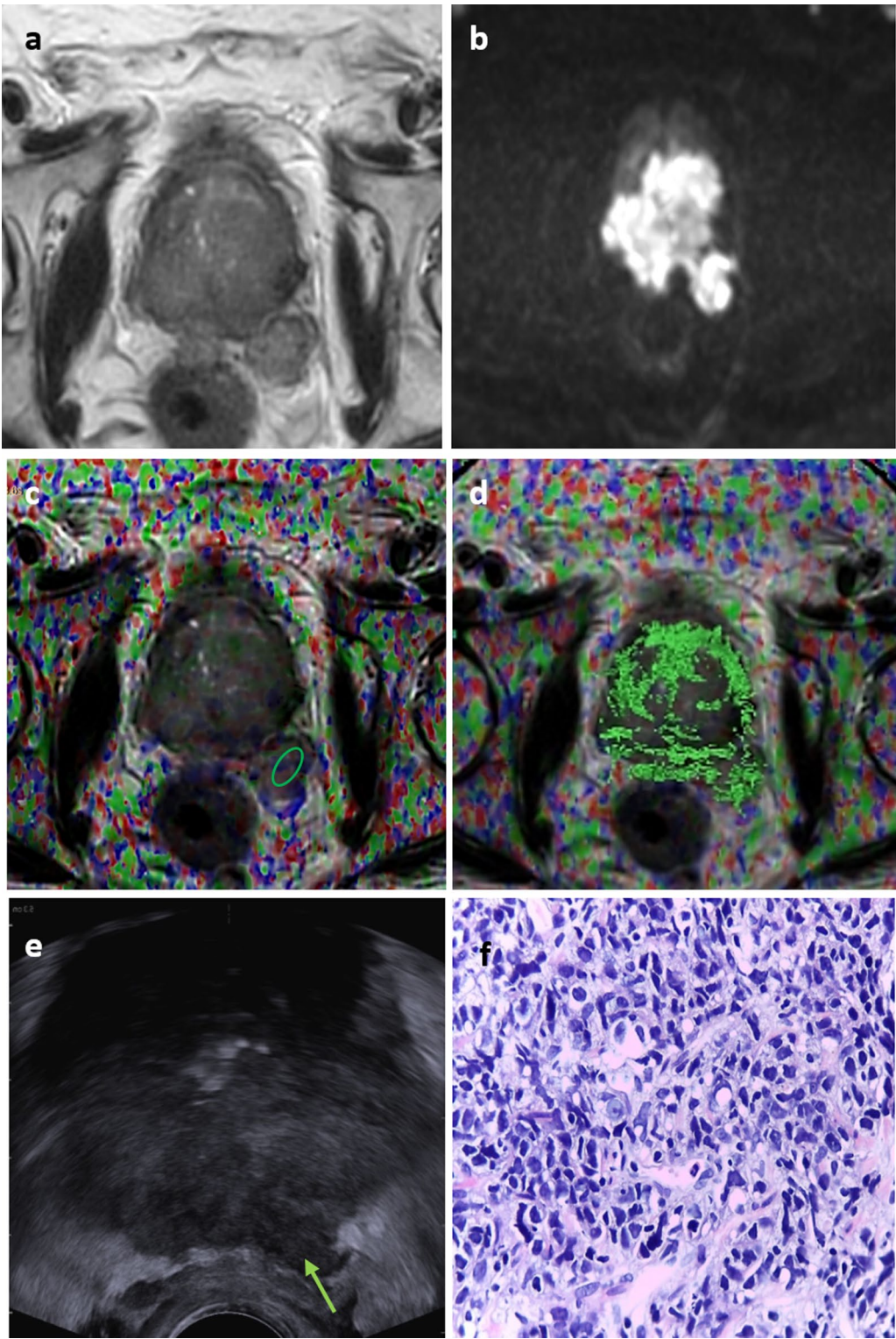


Fig. 7 (See legend on previous page.)

out in a single-center study, on one type of MRI scanner. It is well known that diffusion imaging, including DTI, is very dependent on the scanner type as well as the imaging protocol and modeling.

In conclusion

The results of this research showed that there was a significant correlation between MD and FA values, obtained from DTI and the GS in PCa. So, combined quantitative parameter values (FA and MD values) and parametric diagrams (FA and DTI maps) can be utilized to evaluate prostate cancer aggressiveness, and prognosis, helping in the improvement of the management protocol.

Abbreviations

PCa: Prostate cancer; GS: Gleason score; DTI: Diffusion tensor imaging; FA: Fractional anisotropy; MD: Mean diffusivity; AUC: Area under curve; PSA: Prostate-specific antigen; TRUS: Transrectal ultrasound; DWI: Diffusion weighted imaging; BPH: Benign prostatic hyperplasia; SI: Signal intensity; ROI: Region of interest; SD: Standard deviation; ROC: Receiver operating characteristic; PPV: Positive predictive value; NPV: Negative predictive value; BPH: Benign prostatic hyperplasia.

Acknowledgements

Not applicable.

Author contributions

RA, YA, and ST are responsible as the guarantor of integrity of the entire study. Study concept and design were performed by RA and ST. RA and YA were involved in clinical studies. RA and YA helped in experimental studies/data analysis. RA and YA contributed to statistical analysis. Manuscript preparation was performed by RA and ST. RA and ST helped in manuscript editing. All authors read and approved the final manuscript.

Funding

No funding was obtained for this study.

Availability of data and materials

Due to privacy regulations, the clinical data collected in this study are not deposited in a public registry, but the data can be made available via a request to the corresponding author.

Declarations

Ethics approval and consent to participate:

The Institutional research board of faculty of medicine, University of Mansoura, approved the study (proposal code: MS.19.07.735). A written consent was obtained from the study participants to participate. It was approved by the ethics committee.

Consent for publication

A written consent to publish this information was obtained from study participants.

Competing interests

The authors declare that they have no competing interests, and no relationships with any companies, whose products or services may be related to the subject matter of the article.

Author details

¹Radiology Department, Urology and Nephrology Center, Mansoura University, Mansoura, Egypt. ²Radiology Department, Faculty of Medicine, Mansoura University, Mansoura, Egypt.

Received: 11 August 2022 Accepted: 5 September 2022

Published online: 14 September 2022

References

- Sung H, Ferlay J, Siegel RL et al (2021) Global cancer statistics 2020: GLOBOCAN estimates of incidence and mortality worldwide for 36 cancers in 185 countries. *CA Cancer J Clin* 71(3):209–249. <https://doi.org/10.3322/caac.21660>
- Han C, Liu S, Qin X et al (2020) MRI combined with PSA density in detecting clinically significant prostate cancer in patients with PSA serum levels of 4~10 ng/mL: Biparametric versus multiparametric MRI. *Diagn Interv Imaging* 101(4):235–244. <https://doi.org/10.1016/j.diii.2020.01.014>
- Li L, Margolis DJ, Deng M et al (2015) Correlation of gleason scores with magnetic resonance diffusion tensor imaging in peripheral zone prostate cancer. *J Magn Reson Imaging* 42(2):460–467. <https://doi.org/10.1002/jmri.24813>
- Drost FJH, Osses DF, Nieboer D et al (2019) Prostate MRI, with or without MRI-targeted biopsy, and systematic biopsy for detecting prostate cancer. *Cochrane Database Syst Rev*. <https://doi.org/10.1002/14651858.CD012663.pub2>
- Jellison BJ, Field AS, Medow J et al (2004) Diffusion tensor imaging of cerebral white matter: a pictorial review of physics, fiber tract anatomy, and tumor imaging patterns. *Am J Neuroradiol* 25(3):356–369
- Gholizadeh N, Greer PB, Simpson J et al (2019) Characterization of prostate cancer using diffusion tensor imaging: a new perspective. *Eur J Radiol* 110:112–120. <https://doi.org/10.1016/j.ejrad.2018.11.026>
- Hectors SJ, Semaan S, Song C, et al (2018) Advanced diffusion-weighted imaging modeling for prostate cancer characterization: correlation with quantitative histopathologic tumor tissue composition—a hypothesis-generating study. *Radiology* 286(3):918–928. <https://doi.org/10.1148/radiol.2017170904>
- Gürses B, Tasdelen N, Yencilek F et al (2011) Diagnostic utility of DTI in prostate cancer. *Eur J Radiol* 79(2):172–176. <https://doi.org/10.1016/j.ejrad.2010.01.009>
- Li C, Chen M, Li S et al (2014) Detection of prostate cancer in peripheral zone: comparison of MR diffusion tensor imaging, quantitative dynamic contrast-enhanced MRI, and the two techniques combined at 30 T. *Acta Radiologica* 55(2):239–247. <https://doi.org/10.1177/0284185113494978>
- Shenhar C, Degani H, Ber Y et al (2021) Diffusion is directional: innovative diffusion tensor imaging to improve prostate cancer detection. *Diagnostics* 11(3):563. <https://doi.org/10.3390/diagnostics11030563>
- Hernández J, Thompson IMJ (2004) Prostate-specific antigen: a review of the validation of the most commonly used cancer biomarker. *Cancer* 101(5):894–904. <https://doi.org/10.1002/cncr.20480>
- Mottet N, van den Bergh N, Briers E et al (2021) EAU-EANM-ESTRO-ESUR-SIOG guidelines on prostate cancer—2020 update Part 1: screening, diagnosis, and local treatment with curative intent. *Eur Urol* 79(2):243–262. <https://doi.org/10.1016/j.eururo.2020.09.042>
- Epstein JI, Feng Z, Trock BJ et al (2012) Upgrading and downgrading of prostate cancer from biopsy to radical prostatectomy: incidence and predictive factors using the modified Gleason grading system and factoring in tertiary grades. *Eur Urol* 61(5):1019–1024. <https://doi.org/10.1016/j.eururo.2012.01.050>
- Short E, Warren AY, Varma M (2019) Gleason grading of prostate cancer: a pragmatic approach. *Diagn Histopathol* 25(10):371–378. <https://doi.org/10.1016/j.mpdhp.2019.07.001>
- Weinreb JC, Barentsz JO, Choyke PL et al (2016) PI-RADS prostate imaging—reporting and data system: 2015, version 2. *Eur Urol* 69(1):16–40. <https://doi.org/10.1016/j.eururo.2015.08.052>
- Arif M, Schoots IG, Castillo Tovar J et al (2020) Clinically significant prostate cancer detection and segmentation in low-risk patients using a convolutional neural network on multi-parametric MRI. *Eur Radiol* 30(12):6582–6592. <https://doi.org/10.1007/s00330-020-07008-z>
- Tian W, Zhang J, Tian F et al (2018) Correlation of diffusion tensor imaging parameters and Gleason scores of prostate cancer. *Exp Therapeut Med* 15(1):351–356. <https://doi.org/10.3892/etm.2017.5363>
- Russo AL, Chen MH, Aizer AA et al (2012) Advancing age within established Gleason score categories and the risk of prostate cancer-specific

- mortality (PCSM). *BJU Int* 110(7):973–979. <https://doi.org/10.1111/j.1464-410X.2012.11470.x>
19. Anderson CB, Sternberg IA, Karen-Paz G et al (2015) Age is associated with upgrading at confirmatory biopsy among men with prostate cancer treated with active surveillance. *J Urol* 194(6):1607–1611. <https://doi.org/10.1016/j.juro.2015.06.084>
 20. Vaidyanathan V, Karunasinghe N, Javed A et al (2016) Prostate cancer: Is it a battle lost to age? *Geriatrics* 1(4):27. <https://doi.org/10.3390/geriatrics1040027>
 21. Di Trani MG, Nezzo M, Caporale AS et al (2019) Performance of diffusion kurtosis imaging versus diffusion tensor imaging in discriminating between benign tissue, low and high Gleason grade prostate cancer. *Acad Radiol* 26(10):1328–1337
 22. Onay A, Ertas G, Vural M et al (2017) Evaluation of peripheral zone prostate cancer aggressiveness using the ratio of diffusion tensor imaging measures. *Contrast Media Mol Imaging*. <https://doi.org/10.1016/j.acra.2018.11.015>
 23. Gity M, Moradi B, Arami R et al (2018) Two different methods of region-of-interest placement for differentiation of benign and malignant breast lesions by apparent diffusion coefficient value. *Asian Pac J Cancer Prev* 19(10):2765–2770. <https://doi.org/10.22034/APJCP.2018.19.10.2765>
 24. Ueno Y, Tamada T, Sofue K et al (2022) Do the variations in ROI placement technique have influence for prostate ADC measurements? *Acta Radiol* 11(3):20584601221086500. <https://doi.org/10.1177/20584601221086500>
 25. Wang S, Kim S, Melhem ER (2014) Diffusion tensor imaging: Introduction and applications to brain tumor characterization. In: Pillai JJ (ed) *Functional brain tumor imaging*. Springer, New York p, pp 27–38
 26. Manenti G, Cariani M, Mancino S et al (2007) Diffusion tensor magnetic resonance imaging of prostate cancer. *Invest Radiol* 42(6):412–419. <https://doi.org/10.1097/01.rli.0000264059.46444.bf>
 27. Nezzo M, Di Trani M, Caporale A et al (2016) Mean diffusivity discriminates between prostate cancer with grade group 1&2 and grade groups equal to or greater than 3. *Eur J Radiol* 85(10):1794–1801. <https://doi.org/10.1016/j.ejrad.2016.08.001>
 28. Thompson IM, Ankerst DPJC (2007) Prostate-specific antigen in the early detection of prostate cancer. *Can Med Assoc* 176(13):1853–1858. <https://doi.org/10.1503/cmaj.060955>
 29. Nogueira L, Corradi R, Eastham JAJLbju, (2009) Prostatic specific antigen for prostate cancer detection. *Int Braz J Urol* 35(5):521–531. <https://doi.org/10.1590/s1677-55382009000500003>

Publisher's Note

Springer Nature remains neutral with regard to jurisdictional claims in published maps and institutional affiliations.

Submit your manuscript to a SpringerOpen[®] journal and benefit from:

- Convenient online submission
- Rigorous peer review
- Open access: articles freely available online
- High visibility within the field
- Retaining the copyright to your article

Submit your next manuscript at ► [springeropen.com](https://www.springeropen.com)